

WildRefer: 3D Object Localization in Large-scale Dynamic Scenes with Multi-modal Visual Data and Natural Language

Zhenxiang Lin¹, Xidong Peng¹, Peishan Cong¹, Yuenan Hou²,
Xinge Zhu³, Sibe Yang¹, Yuexin Ma¹

¹ShanghaiTech University, ²Shanghai AI Laboratory, ³The Chinese University of Hong Kong
zhenxiang.lin@unswalumni.com, {pengxd, pcongsh, yangsb, mayuexin}@shanghaitech.edu.cn,
houyuenan@pjlab.org.cn, zhuxinge123@gmail.com

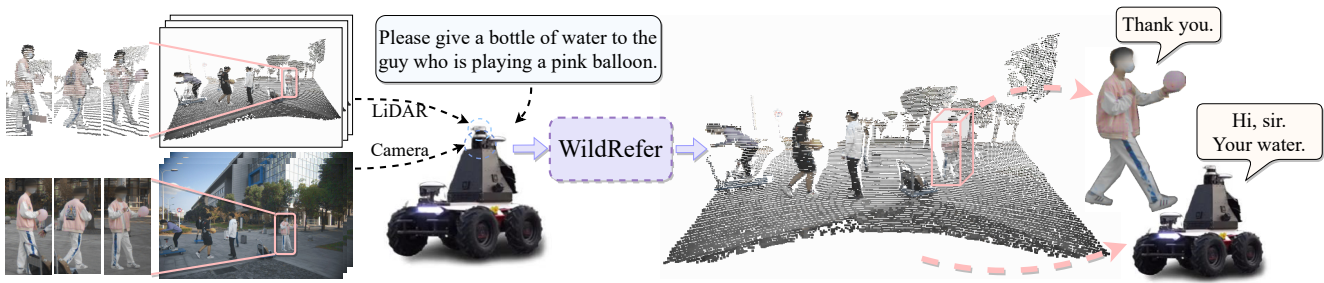


Figure 1. Introduction for 3DVGW task and related application. The robot observes the dynamic scene and locates the 3D object according to natural language description. Then, the robot moves to service the target object. WildRefer provides a LiDAR-camera multi-sensor-based solution, which can conduct 3D visual grounding in large-scale free environment.

Abstract

We introduce the task of 3D visual grounding in large-scale dynamic scenes based on natural linguistic descriptions and online captured multi-modal visual data, including 2D images and 3D LiDAR point clouds. We present a novel method, WildRefer, for this task by fully utilizing the appearance features in images, the location and geometry features in point clouds, and the dynamic features in consecutive input frames to match the semantic features in language. In particular, we propose two novel datasets, STRefer and LifeRefer, which focus on large-scale human-centric daily-life scenarios with abundant 3D object and natural language annotations. Our datasets are significant for the research of 3D visual grounding in the wild and has huge potential to boost the development of autonomous driving and service robots. Extensive comparisons and ablation studies illustrate that our method achieves state-of-the-art performance on two proposed datasets. **Code and dataset will be released when the paper is published.**

1. Introduction

Human has the ability to parse the dynamic scene and localize the object with semantic understanding in real time, which enables us to carry out specific tasks, like helping the elderly up who fell or serving the lady who is dancing with a cup of tea. In this paper, we propose a new task, *3D Visual Grounding in the Wild (3DVGW)*, which aims at locating a desired object in the real world via online captured visual data and object-oriented linguistic description, like Figure. 1 shows. It is significant for many downstream applications, such as assistive robots, autonomous driving, security, etc.

In recent years, 2D visual grounding has achieved great progress [49, 46, 31, 47, 13] based on many large-scale datasets [50, 33, 29, 24, 12]. However, these methods and datasets are limited to 2D images, which are hard to be extended to 3D applications directly. To capture the 3D geometry features of objects and spatial relationships among objects for 3D visual grounding, some works [6, 1, 51, 52, 15, 5, 32, 21] propose related datasets and solutions to localize 3D objects in RGB-D scans according to natural language descriptions, which are meaningful for the robotic manipulation and augmented reality. However, RGB-D camera can

only work in indoor scenarios with 5m available sensing range and these methods focus on pre-scanned indoor static scenarios, which are limited for 3D grounding in dynamic large-scale scenes with online captured visual data.

To capture long-range scenes in free environment, we leverage calibrated and synchronized LiDAR and camera as visual sensors, which are usually adopted by outdoor robots and autonomous vehicles [4, 3, 55]. 3DVGW differs from previous RGB-D-based visual grounding in two aspects, including dynamic scenarios and multi-modal visual data. For the dynamic real world, motion-related language descriptions are commonly used and temporal information in visual data is worth exploring for more accurate vision-language matching. For multi-modal visual data, LiDAR point clouds contain 3D geometry and location information and images include rich appearance pattern, an effective and efficient sensor-fusion strategy is thus necessary to make them complement each other and further benefit the visual grounding task.

Taking these issues into consideration, we propose a novel approach, namely **WildRefer**, for 3DVGW based on LiDAR-camera multi-visual sensors. First, we design a **Dynamic Visual Encoder** to extract the motion feature from consecutive visual data. Actually, the location, pose, and appearance features of objects may vary over time, it is non-trivial to track the changes belonging to the same object. We apply a transformer-based mechanism to match corresponding sequential features automatically. Second, we design a **Triple-modal Feature Interaction** module to make the semantic information in language, the geometry information in point clouds, and the appearance information in images interact with each other to enhance the representation of both linguistic and visual features. Finally, similar as [21], we adopt a DETR-form decoder to predict bounding boxes of objects and conduct the selection for target through contextualized features of language utterance and visual tokens.

To facilitate the research of 3DVGW, we propose two new datasets, STRefer and LifeRefer, which are captured in large-scale human-centric scenarios by an 128-beam mechanical LiDAR and an industrial camera. STRefer is extended from the open-source dataset STCrowd [11], which targets for 3D perception task in crowd scenarios. We sample 662 LiDAR scans and synchronized images and add 5,458 free-form language descriptions. LifeRefer is newly collected in various daily-life scenes with rich human activities, human-human interactions, and human-object interactions. It contains 25,380 natural language descriptions for 11,864 subjects from 3,172 scenes. Human-centric free environment is much more complex than static indoor scenes or traffic scenes, which is challenging but significant for the development of autonomous driving and service robots. Our datasets fill the blank of data in this field and have po-

tential to boost related research. In particular, our method is evaluated on both datasets by extensive experiments and achieve state-of-the-art performance.

Our contributions can be summarized as follows:

- We introduce the task of 3D vision grounding in the wild, where the scene is large-scale and dynamic and the visual data is online captured by multiple sensors.
- We provide two novel datasets for 3DVGW, which are captured in human-centric scenarios, containing multi-modal visual data and human-written natural language descriptions.
- We propose a novel method for 3DVGW, where temporal information is fully explored and multi-modal features are fused effectively for accurate target localization.

2. Related Works

2.1. 2D Visual Grounding

There are already a lot of investigations about image-based or video-based 2D visual grounding task. To handle this task, a number of datasets [50, 33, 24, 12, 53, 39] are created by asking the annotators to provide expressions for specific image regions, and many methods [9, 19, 22, 54] are proposed subsequently. Some approaches are based on the two-stage architecture [34, 49, 46, 18, 44] by detecting all potential objects from the image, and then locating the target object according to the referring expression. Inspired by traditional one-stage detection methods, one-stage grounding approaches [47, 27, 48] appear by fusing image and language features densely and locating the target directly. With the success of transformer [42] and BERT [14], recently, some researchers [31, 41, 13] apply these frameworks on the visual grounding problem and achieve promising performance. However, due to the lack of depth and 3D geometry information in images, these 2D visual grounding approaches cannot be extended to 3D scenes directly.

2.2. 3D Visual Grounding

To facilitate the development of artificial intelligence in 3D real scenes, 3D visual grounding has gained more and more attention. Scanrefer [6] is the first indoor 3D grounding dataset based on RGB-D scans and natural language descriptions. Afterwards, [1] propose Nr3d and Sr3d datasets according to different language forms. These datasets stimulate the progress of visual grounding in 3D scenes. [51] uses instance-level information to enhance the location. [20] uses multiple views to improve the robustness. [52] proposes a new framework which takes more attention on spatial relation among point clouds. [5] designs a unified framework to solve both visual captioning and

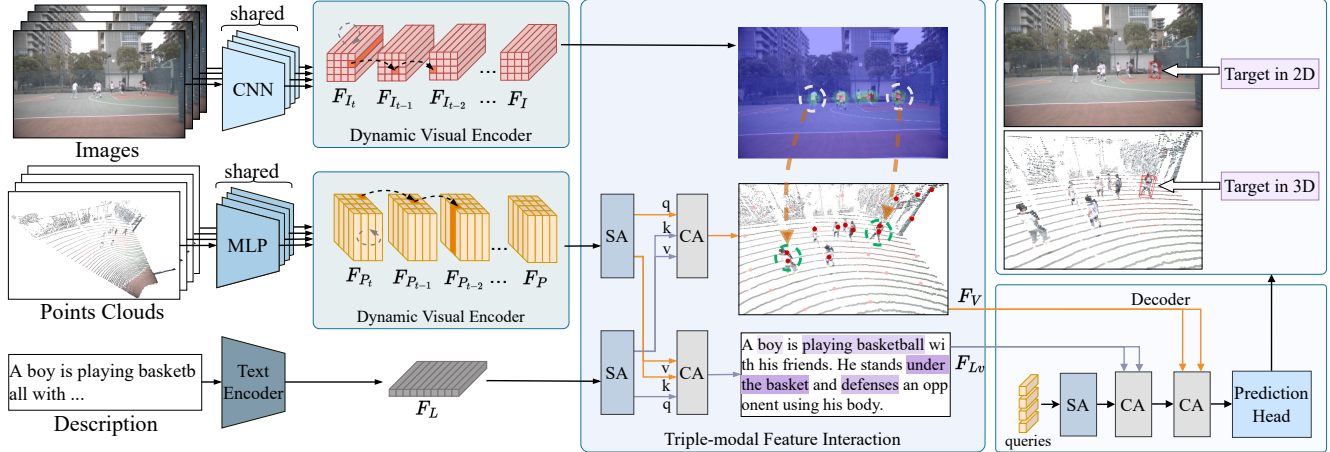


Figure 3. Pipeline of WildRefer. The inputs are multi-frame synchronized points clouds and images as well as a natural language description. After feature extraction, we obtain two types of visual feature and a text feature. Through two dynamic visual encoders, we extract dynamic-enhanced image and point features. Then, a triple-modal feature interaction module is followed to fuse valuable information from different modalities. Finally, through a DETR-like decoder, we decode the location and size of the target object. SA and CA denote self-attention and cross-attention, respectively.

for accurate 3D localization. For both datasets, the visual data are captured by calibrated and synchronized 10Hz 128-beam Ouster-OS1 LiDAR and industrial camera with 1920×1200 image resolution.

3.2. Annotations

For each target object, we provide a free-form linguistic description and a 3D bounding box. The 3D bounding box is represented by $(x, y, z, l, w, h, \theta)$, where x, y, z denotes the center in the LiDAR coordinates system, l, w, h represents the size of box, and θ is the orientation. To ensure the free-form descriptions, we organize ten persons with different genders and ages to the label language without any limitation of expression styles. To guarantee the correctness and uniqueness of the linguistic description for target objects, we implement a triple-check mechanism. For each description of one annotator, only the one that three other annotators all correctly localize the target in the scene can remain.

3.3. Statistics

We uniformly sampled 662 scenes from original STCrowd dataset for **STRefer** and annotate 5,458 natural language descriptions for 3,581 subjects. The scene here means a frame of synchronized LiDAR point cloud and image. The content in each scene distinguishes from others due to changing capture locations or time. We split it into training and testing data by 4:1 without data leakage. **LifeRefer** involves 25,380 natural language descriptions for 11,864 subjects based on 3,172 scenes. Similarly, we split it into 14,650 training data and 10,730 testing data without data leakage. For both datasets, we ensure each word in

the test set appears at least twice in the training set to avoid the influence of data randomness on the experiment. Figure. 2 shows commonly used attributes in our descriptions. We also provide the consecutive neighboring frames of raw data for each scene to benefit the leverage of dynamic information. In particular, all the faces in images are masked for **privacy-preserving**.

3.4. Characteristics

Compared with existing open-source datasets for 3D visual grounding, STRefer and LifeRefer have four unique characteristics, listed in Table. 1. Detailed analyses are as follows.

Human-centric scene understanding. Scene understanding for static indoor scenarios and traffic scenarios have made great progress in recent years, which truly boosts the development of autonomous driving and assistive robots. Human-centric scene understanding progresses relatively slowly due to the lack of large-scale open datasets and the intrinsic difficulties of the problem, where humans have abundant poses, actions, and interaction with other humans or objects. Our datasets focus on the challenging human-centric scenarios, which is significant for developing fine-grained interactive robots.

Large-scale Dynamic Scenes with Time Series. We are living in a dynamic world with moving and changing objects and environments. Our datasets concern the real large-scale dynamic scenes and capture consecutive visual data. When annotating the language for targets, we also pay attention to the description for temporal states, such as short-term or long-term actions. The sequential visual data and time series dependent linguistic descriptions is a distin-

guishing feature of our datasets.

Multi-modal Visual Data. RGB-D camera can only work in indoor scenarios with 5m perception range. To capture the long-range scene data, the popular configuration of visual sensor is the calibrated LiDAR and camera, which provide 3D point cloud and 2D images, respectively. We follow this setting in our dataset to facilitate the downstream robotic applications. However, compared with RGB-D data, the LiDAR point cloud is unordered and much sparser and there are no accurate one-to-one physical correspondence between it and images. Therefore, the fusion strategy of unordered-sparse represented point cloud and regular-dense represented image is not straightforward, which all bring challenges to accurate object grounding.

View-dependency. For the aim of real-time grounding in the wild, we use online captured visual data, which is different from the pre-scanned point cloud of whole scenes [6, 1]. It is similar to human’s observation, where external and self-occlusions exist in crowded scenarios. The benefit is that all spatial relations in our descriptions are all based on the sensor view, which is much clearer than the definition in the global view and is more suitable for application deployment.

4. Methodology

4.1. Overview

For our 3DVGW task, the inputs include synchronized LiDAR points clouds and images as well as one free-form linguistic description. The output is the 3D bounding box of the target object in physical world. To fully exploit the temporal information existing in sequential data and match with action-related descriptions, we design a useful dynamic visual feature encoder. Moreover, in order to make both the geometry information in point clouds and appearance pattern in images better align with the semantic feature in language, we propose a triple-modal feature interaction strategy for feature enhancement. As shown in Figure. 3, our method, WildRefer, solves the 3DVGW problem in the one-stage fashion, including initial feature extractors, a dynamic visual encoder (DVE), a triple-modal feature interaction module (TFI), and a decoder. We introduce details of our method in the following.

4.2. Feature extraction

We use pointnet++ [38] to extract the geometry features $\{F_{P_t}, F_{P_{t-1}}, F_{P_{t-2}}, \dots, F_{P_{t-K+1}}\}$ from temporal point clouds and pretrained ResNet34 [17] to extract appearance features $\{F_{I_t}, F_{I_{t-1}}, F_{I_{t-2}}, \dots, F_{I_{t-K+1}}\}$ from temporal images, where subscripts t and $t - 1$ denote the data of current and previous time, and K denotes the length of input sequence. For utterances, we leverage pretrained RoBERTa [35] to extract text feature F_L .

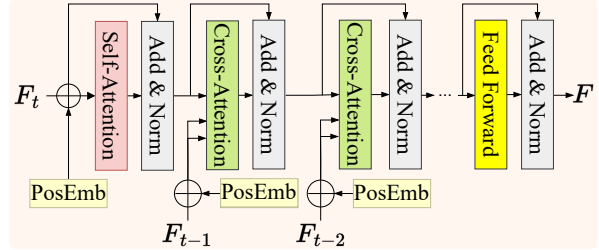


Figure 4. Structure of dynamic visual encoder. F indicates the feature extracted from either LiDAR points cloud or images, t denotes the time, and PosEmb means position embedding.

4.3. Dynamic Visual Encoder (DVE)

Apart from location or texture related descriptions, dynamic motion-related descriptions are also important signals to locate specific human target in large-scale scenes, such as walking, standing, sitting, riding, waving, etc. Moreover, the occlusion problem in dense crowd can also be alleviated by using temporal information. Such dynamic features can be extracted from consecutive visual data, where the changes of depth values in points clouds and pixel values in images represent motion patterns of human actions. Because the scene content is always changing, it is not easy to match the object features from different times in large-scale scenes. Therefore, we apply a spatial-temporal attention mechanism to track critical features for objects automatically. As shown in Figure. 4, we first enhance the spatial feature of current time by self-attention. And then, by gradually matching the feature from previous time series through cross-attention, we obtain the dynamic feature F of object. The process for utilizing two consecutive frames is

$$ATT(q, k, v) = softmax\left(\frac{q \cdot k}{\sqrt{C}}\right) \cdot v,$$

$$F' = ATT(F_t, F_{t-1} + P_{t-1}, F_{t-1} + P_{t-1}), \quad (1)$$

$$F = LN(FFN(F') + F'),$$

where P_{t-1} denotes the position embedding at $t - 1$ time, LN is layer normalization, FFN means feed forward layer.

4.4. Triple-modal Feature Interaction (TFI)

At current time, we already have one semantic feature F_L from language and two dynamic visual features F_P and F_I from point clouds and images. We make these triple-modal features cross-attend with each other to benefit the vision-language matching and target localization.

For the visual grounding task in 3D space, the visual feature of point cloud contains rich geometry, position, and motion information, which are critical to match with language descriptions. Moreover, the 3D coordinate-related representation of point feature is also the key for the final

Table 2. Comparison of 3D visual grounding methods on STRefer and LifeRefer. BUTD-DETR* is the one-stage version without using pretrained object decoder.

Method	Publication	Type	STRefer			LifeRefer			Time cost (ms)
			Acc@0.25	Acc@0.5	mIOU	Acc@0.25	Acc@0.5	mIOU	
ScanRefer [6]	ECCV-2020	Two-Stage	32.93	30.39	25.21	22.76	14.89	12.61	156
ReferIt3D [1]	ECCV-2020	Two-Stage	34.05	31.61	26.05	26.18	17.06	14.38	194
3DVG-Transformer [52]	ICCV-2021	Two-Stage	40.53	37.71	30.63	25.71	15.94	13.99	160
MVT [20]	CVPR-2022	Two-Stage	45.12	42.40	35.03	21.65	13.17	11.71	242
3DJCG [5]	CVPR-2022	Two-Stage	50.47	47.47	38.85	27.82	16.87	15.40	161
BUTD-DETR [21]	ECCV-2022	Two-Stage	57.60	47.47	35.22	30.81	11.66	14.80	252
BUTD-DETR* [21]	ECCV-2022	One-Stage	56.66	45.12	33.52	32.46	12.82	15.96	138
3D-SPS [32]	CVPR-2022	One-Stage	44.47	42.40	30.43	28.01	18.20	15.78	130
Ours	–	One-Stage	62.29	52.72	38.25	38.88	18.43	19.47	151

target localization. Therefore, we first make the point feature interact with the language feature via a sequence of cross-attention layers, like Figure. 3 shows. The process is represented by Formula. 2. After this, we obtain visual-enhanced semantic feature F_{Lv} and the semantic-enhanced point feature F_{Pl} .

$$\begin{aligned} F_{Lv} &= LN(FFN(ATT(F_L, F_P, F_P) + F_L)). \\ F_{Pl} &= LN(FFN(ATT(F_P, F_L, F_L) + F_P)). \end{aligned} \quad (2)$$

Then, we further enhance the point feature through fusing corresponding dense texture features from images. Because there are no strict one-to-one physical correspondence between 2D and 3D features, we make use of cross-attention to learn effective fusion strategy automatically. Finally, the comprehensive visual feature F_V is calculated by

$$F_V = ATT(F_{Pl}, F_I, F_I). \quad (3)$$

4.5. Decoder

Similar to BUTD-DETR[21], we use non-parametric queries, selected by N highest confidences s . The confidence score is obtained by F_V through a MLP. Then, through cross attention, the queries gradually extract key information from semantic feature and visual feature. Next, the prediction head decodes the location and size of the objects, and a $N \times M$ probability mapping of each visual token and each word in the utterance, where M is the length of the sentence. Finally, we select the bounding box whose corresponding visual feature is furthest with word feature of “not-mentioned” as the target location.

4.6. Training Details

We use five distinct losses to supervise our training process. Firstly, we use focal loss L_s to supervise the target confidence s to increase the distribution difference between target points and non-target points. Then, we use GIoU loss L_{giou} and L1 loss L_{box} to supervise the position and size of predicted boxes. Following [21], we use a contrastive loss L_c to supervise the similarity of visual tokens and their

corresponding word feature. The visual feature of the target should be similar with the semantic feature of target word in the utterance and different with other words. The structure of sentence is parsed by SpaCy. In addition, one span “not-mentioned” is appended at the end of utterances to match non-target objects queries. At last, we use soft token prediction loss [22] L_{st} to supervise the probability mapping of each visual tokens and words. Finally our loss L is calculated by

$$L = \alpha L_s + \beta L_{giou} + \gamma L_{box} + \lambda L_c + \mu L_{st}, \quad (4)$$

where $\alpha, \beta, \gamma, \lambda$ and μ are weights of losses.

5. Experiments

In this section, we first provide implementation details and evaluation metrics, and then show extensive experiments, including the comparison with current state-of-the-art methods and ablation studies.

5.1. Implementation Details

Feature extractor. We use ResNet34 [17] and PointNet++ [38] to extract visual features, and RoBERTa [35] to extract language features. All features are projected to 288-D.

Hyper-parameters. We use 1-layer and 6-layer transformers in the DVE and decoder, respectively. For the cross-attention in TFI, we set 3 layers. We extract dynamic features from consecutive two frames (spanning one second) of data. For all layers in the transformer, we use 8-head attention and 256-D feed-forward layer with 10% dropout.

Training stage. We train 200 epochs on STRefer and 60 epochs on LifeRefer by AdamW [30] with 0.0001 learning rate and 0.0005 weight decay. For PointNet++[38] and RoBERTa [35], the initial learning rates are 0.001 and 0.00001. The learning rate decays by a factor of 10 after 45 epochs on LifeRefer. The weights of losses $\alpha, \beta, \gamma, \lambda$ and μ are set as 8, 1, 5, 1 and 0.01.

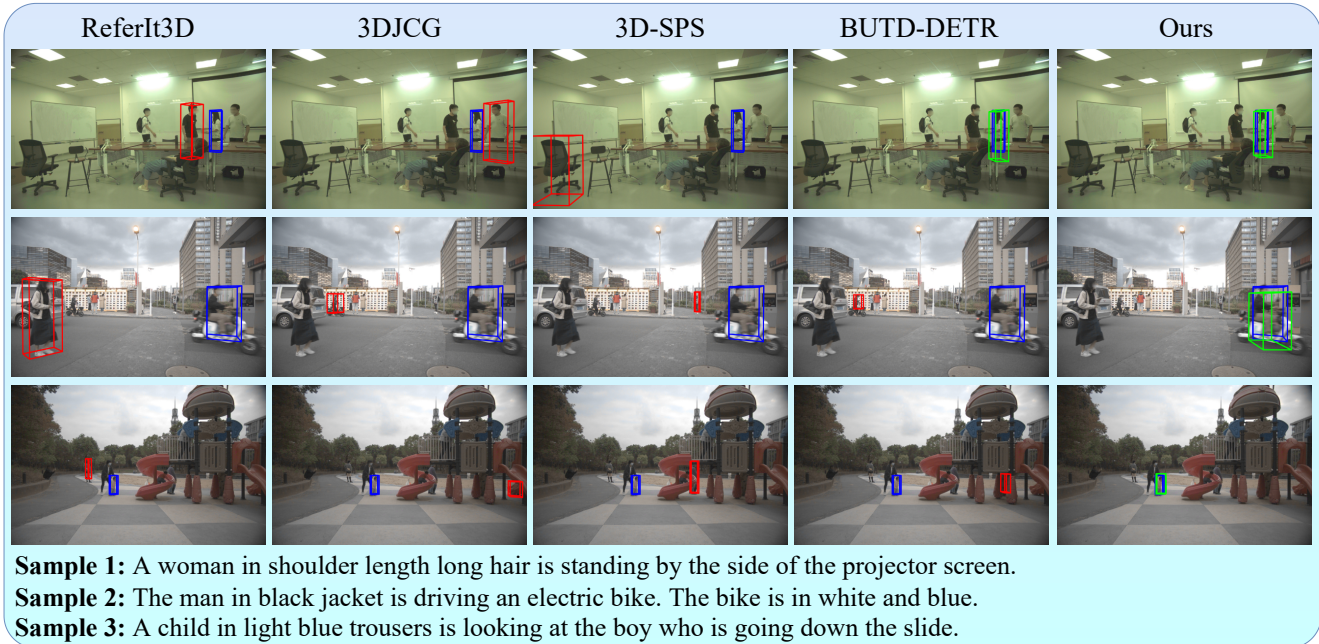


Figure 5. Visualization of comparison results on LifeRefer. Blue, red, and green boxes denote the ground truth, wrong prediction, and right prediction, respectively.

Table 3. 3D Detection performance on STRefer and LifeRefer. We show precision (P) and recall (R) with 25% and 50% IOU.

	R@0.25	R@0.5	P@0.25	P@0.5
STRefer	90.77	82.13	91.69	83.01
LifeRefer	77.11	43.16	60.09	33.63

5.2. Evaluation Metrics

We use the accuracy with 3D IOU threshold and mean IOU (mIOU) as metrics and choose 0.25 and 0.5 as IOU thresholds. They are calculated by Formula. 5, where $|\Omega|$ is the number of samples in dataset.

$$Acc(IOU_{thr}) = \frac{1}{|\Omega|} \sum_{i=1}^{|\Omega|} I(IOU_i \geq IOU_{thr}), \quad (5)$$

$$mIOU = \frac{1}{|\Omega|} \sum_{i=1}^{|\Omega|} IOU_i.$$

Table 4. Ablation studies of our method on STRefer and LifeRefer.

		Acc@0.25	Acc@0.5	mIOU
STRefer	baseline	56.66	45.12	33.52
	+ DVE	59.76	50.28	36.59
	+ DVE + TFI	62.29	52.72	38.25
LifeRefer	baseline	32.46	12.82	15.96
	+ DVE	38.27	16.42	18.83
	+ DVE + TFI	38.88	18.43	19.47

5.3. Comparison

Because we are the first to solve 3DVGW task based on multi-sensor visual data in dynamic scenes, there is no related work for absolutely fair comparison. In order to verify the effectiveness of our method, we compare with recent SOTA methods for 3D visual grounding based on RGB-D scans, including ScanRefer [6], ReferIt3D [1], 3DVG-Transformer [52], Multi-View Transformer (MVT) [20], 3DJCG [5], 3D-SPS [32] and BUTD-DETR [21] as Table. 2 shows. To achieve fair comparisons as much as possible, we project the LiDAR point cloud on the image by calibration metrics and paint points with the corresponding color on the image to obtain the pseudo RGB-D data. We conduct experiments by using their released code. For two-stage methods, we use current state-of-the-art 3D detector [11] pretrained on STCrowd and LifeRefer to provide 3D proposals in the first stage. The detection performance is shown in Table. 3. Because BUTD-DETR can run without pre-detection inputs, we also run a one-stage BUTD-DETR for the comparison.

It can be seen from the results that our method outperforms others obviously. Previous 3D visual grounding methods rely on RGB-D representation where points and colors have physical dense correspondence. While for the LiDAR and camera setting, direct painting colors on sparse LiDAR point cloud will miss lots of texture features in images. Our method utilizes cross-attention to learn valuable features from different modalities for fusion, keeping more critical visual information for the further vision-language

matching. Furthermore, our one-stage framework can get rid of the dependence on 3D detector. From Table. 3, we can see that scenarios in LifeRefer is much more complex than that of STRefer, causing low detection accuracy. An interesting phenomenon is that the one-stage version of BUTD-DETR is superior than its two-stage version due to the low-quality detected proposals. Although two-stage methods have more prior knowledge by pretraining with more data for supervision, one-stage framework still achieves better performance especially for in-the-wild complex scenarios. Moreover, our method extracts dynamic features of real scenes, which can better match motion-related descriptions for more accurate localization. In addition, we also show the time cost of inference in Table. 2. Although our method is required to process multi-frame data and using transformer mechanism for feature interaction, it is still efficient and has the potential to be applied in real-time applications. The qualitative comparison is illustrated in Figure. 5.

5.4. Ablation Studies

We conduct ablation studies to verify the effectiveness of network modules and the multi-modal feature fusion strategy.

5.4.1 Network Modules

Quantitative and qualitative ablation results are demonstrated in Table. 4 and Figure. 6.

Baseline. For the baseline network, we only use one frame of point cloud painted by color as the visual input and only conduct point-language interaction by cross-attention.

Baseline + DVE. The Dynamic Visual Encoder (DVE) is attached after point feature extractor in baseline network to make full use of dynamic information. After spatial-temporal attention, we obtain the motion feature of objects, which is helpful to localize the target by matching the dynamic information in descriptions.

Baseline + DVE + TFI. This is the complete network of our method. Triple-model feature interaction module (TFI) leverage dense appearance features in images to compensate for the shortcomings of sparse point representation. As Figure. 6 shows, the detailed feature “white stripes” cannot be recognized by point cloud-only representation, but can be recognized by fusing two modal visual features.

5.4.2 Multi-modal Fusion Strategy

In our setting, we have three modalities and related features, including the language, point clouds, and images. For locating the target, it is necessary to obtain valuable information for the object from all modal data and conduct accurate mapping from visual feature to linguistic feature. For our triple-modal feature interaction module, we make point feature and language feature interact with each other first and

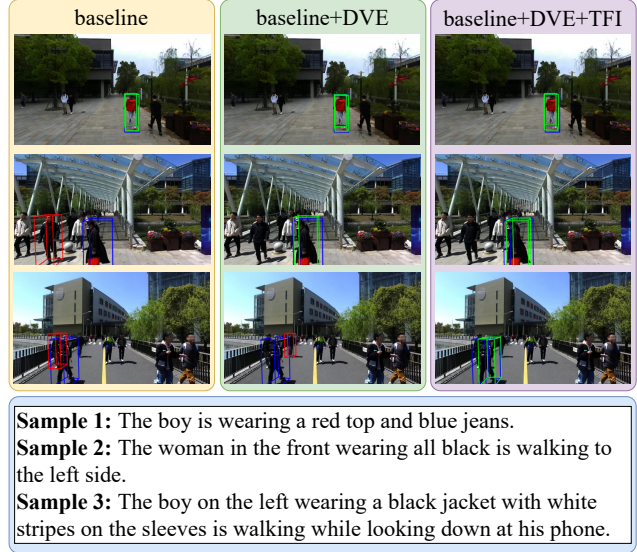


Figure 6. Visualization results of ablation experiments on STRefer. Blue, red, and green boxes denote the ground truth, wrong prediction, and right prediction, respectively.

then fuse image features with the semantic guidance. We compare with other feature-fusion orders in Table. 5.

Vision First. In this setting, we firstly fuse image feature into points feature and then interact with language feature. It can obtain a comparable result but a bit lower than ours, mainly because the fused visual feature is more complicated for language feature to find corresponding information.

Table 5. Comparison of other visual fusion orders.

		Acc@0.25	Acc@0.5	mIOU
STRefer	Vision First	59.74	52.72	37.11
	Image Domin.	52.25	47.47	32.80
	ours	62.69	52.72	38.25
LifeRefer	Vision First	37.27	16.92	18.65
	Image Domin.	38.82	16.78	18.87
	ours	38.88	18.43	19.47

Image Domin. In this setting, we use image as main feature to cross-fuse with language feature first and as queries to extract point clouds feature. The performance drops on STRefer, mainly because we aim to locate targets in 3D space and a point-dominated feature with accurate position information is more suitable than image-dominated feature.

6. Future Work

For our new datasets, they all focus on human targets in large-scale scenarios, which is significant for the development of service robots and intelligent security. However, it is promising to extend them with more comprehensive descriptions for all objects in scenes. By then, complex human-object interactions and human-environment interactions should be considered for accurate 3D localization.

7. Conclusion

In this paper, we first introduce the task of 3DVGW, which focuses on the large-scale dynamic scenes and uses online captured multi-modal visual data. Then, we propose effective vision-language interaction and sensor-fusion strategy for 3D vision grounding by fully utilizing the geometry feature, appearance feature, and motion feature. In particular, we propose two novel datasets for 3DVGW on human-centric scenarios and hope our work could inspire more related research for developing AI robots.

References

- [1] Panos Achlioptas, Ahmed Abdelreheem, Fei Xia, Mohamed Elhoseiny, and Leonidas Guibas. Referit3d: Neural listeners for fine-grained 3d object identification in real-world scenes. In *European Conference on Computer Vision*, pages 422–440. Springer, 2020. 1, 2, 3, 5, 6, 7
- [2] Xuyang Bai, Zeyu Hu, Xinge Zhu, Qingqiu Huang, Yilun Chen, Hongbo Fu, and Chiew-Lan Tai. Transfusion: Robust lidar-camera fusion for 3d object detection with transformers. In *CVPR*, pages 1090–1099, 2022. 3
- [3] Jens Behley, Martin Garbade, Andres Milioto, Jan Quenzel, Sven Behnke, Cyrill Stachniss, and Jurgen Gall. Semantickitti: A dataset for semantic scene understanding of lidar sequences. In *Proceedings of the IEEE/CVF international conference on computer vision*, pages 9297–9307, 2019. 2
- [4] Holger Caesar, Varun Bankiti, Alex H Lang, Sourabh Vora, Venice Erin Liong, Qiang Xu, Anush Krishnan, Yu Pan, Giancarlo Baldan, and Oscar Beijbom. nuscenes: A multi-modal dataset for autonomous driving. In *Proceedings of the IEEE/CVF conference on computer vision and pattern recognition*, pages 11621–11631, 2020. 2
- [5] Daigang Cai, Lichen Zhao, Jing Zhang, Lu Sheng, and Dong Xu. 3djcg: A unified framework for joint dense captioning and visual grounding on 3d point clouds. In *CVPR*, pages 16464–16473, 2022. 1, 2, 6, 7
- [6] Dave Zhenyu Chen, Angel X Chang, and Matthias Nießner. Scanrefer: 3d object localization in rgb-d scans using natural language. In *ECCV*, pages 202–221. Springer, 2020. 1, 2, 3, 5, 6, 7
- [7] Jiaming Chen, Weixin Luo, Xiaolin Wei, Lin Ma, and Wei Zhang. Ham: Hierarchical attention model with high performance for 3d visual grounding. *arXiv preprint arXiv:2210.12513*, 2022. 3
- [8] Xuanyao Chen, Tianyuan Zhang, Yue Wang, Yilun Wang, and Hang Zhao. Futr3d: A unified sensor fusion framework for 3d detection. *arXiv preprint arXiv:2203.10642*, 2022. 3
- [9] Jaemin Cho, Jie Lei, Hao Tan, and Mohit Bansal. Unifying vision-and-language tasks via text generation. In *ICML*, pages 1931–1942. PMLR, 2021. 2
- [10] Peishan Cong, Yiteng Xu, Yiming Ren, Juze Zhang, Lan Xu, Jingya Wang, Jingyi Yu, and Yuexin Ma. Weakly supervised 3d multi-person pose estimation for large-scale scenes based on monocular camera and single lidar. *arXiv preprint arXiv:2211.16951*, 2022. 3
- [11] Peishan Cong, Xinge Zhu, Feng Qiao, Yiming Ren, Xidong Peng, Yuenan Hou, Lan Xu, Ruigang Yang, Dinesh Manocha, and Yuexin Ma. Stcrowd: A multimodal dataset for pedestrian perception in crowded scenes. *CVPR*, 2022. 2, 3, 7
- [12] Harm De Vries, Florian Strub, Sarath Chandar, Olivier Pietquin, Hugo Larochelle, and Aaron Courville. Guess-what?! visual object discovery through multi-modal dialogue. pages 5503–5512, 2017. 1, 2
- [13] Jiajun Deng, Zhengyuan Yang, Tianlang Chen, Wengang Zhou, and Houqiang Li. Transvg: End-to-end visual grounding with transformers. In *ICCV*, pages 1769–1779, 2021. 1, 2
- [14] Jacob Devlin, Ming-Wei Chang, Kenton Lee, and Kristina Toutanova. Bert: Pre-training of deep bidirectional transformers for language understanding. *arXiv preprint arXiv:1810.04805*, 2018. 2
- [15] Mingtao Feng, Zhen Li, and etc. Free-form description guided 3d visual graph network for object grounding in point cloud. In *Proceedings of the IEEE/CVF International Conference on Computer Vision (ICCV)*, pages 3722–3731, October 2021. 1, 3
- [16] Xiao Han, Peishan Cong, Lan Xu, Jingya Wang, Jingyi Yu, and Yuexin Ma. Licamgait: Gait recognition in the wild by using lidar and camera multi-modal visual sensors. *arXiv preprint arXiv:2211.12371*, 2022. 3
- [17] Kaiming He, Xiangyu Zhang, Shaoqing Ren, and Jian Sun. Deep residual learning for image recognition. In *Proceedings of the IEEE Conference on Computer Vision and Pattern Recognition (CVPR)*, June 2016. 5, 6
- [18] Ronghang Hu, Marcus Rohrbach, and etc. Modeling relationships in referential expressions with compositional modular networks. In *CVPR*, pages 1115–1124, 2017. 2
- [19] Jianqiang Huang, Yu Qin, Jiaxin Qi, Qianru Sun, and Hanwang Zhang. Deconfounded visual grounding. *arXiv preprint arXiv:2112.15324*, 2021. 2
- [20] Shijia Huang, Yilun Chen, Jiaya Jia, and Liwei Wang. Multi-view transformer for 3d visual grounding. In *Proceedings of the IEEE/CVF Conference on Computer Vision and Pattern Recognition*, pages 15524–15533, 2022. 2, 6, 7
- [21] Ayush Jain, Nikolaos Gkanatsios, Ishita Mediratta, and Katerina Fragkiadaki. Bottom up top down detection transformers for language grounding in images and point clouds. *CoRR*, abs/2112.08879, 2021. 1, 2, 3, 6, 7
- [22] Aishwarya Kamath, Mannat Singh, and etc. Mdetr-modulated detection for end-to-end multi-modal understanding. In *ICCV*, pages 1780–1790, 2021. 2, 6
- [23] Manuel Kolmet, Qunjie Zhou, Aljoša Ošep, and Laura Leal-Taixé. Text2pos: Text-to-point-cloud cross-modal localization. In *Proceedings of the IEEE/CVF Conference on Computer Vision and Pattern Recognition*, pages 6687–6696, 2022. 3
- [24] Ranjay Krishna, Yuke Zhu, Oliver Groth, Justin Johnson, Kenji Hata, Joshua Kravitz, Stephanie Chen, Yannis Kalantidis, Li-Jia Li, David A Shamma, et al. Visual genome: Connecting language and vision using crowdsourced dense image annotations. *International journal of computer vision*, 123(1):32–73, 2017. 1, 2

- [25] Yingwei Li, Adams Wei Yu, Tianjian Meng, Ben Caine, Jiquan Ngiam, Daiyi Peng, Junyang Shen, Yifeng Lu, Denny Zhou, Quoc V Le, et al. Deepfusion: Lidar-camera deep fusion for multi-modal 3d object detection. In *CVPR*, pages 17182–17191, 2022. [3](#)
- [26] Tingting Liang, Hongwei Xie, Kaicheng Yu, Zhongyu Xia, Zhiwei Lin, Yongtao Wang, Tao Tang, Bing Wang, and Zhi Tang. Bevfusion: A simple and robust lidar-camera fusion framework. *arXiv preprint arXiv:2205.13790*, 2022. [3](#)
- [27] Yue Liao, Si Liu, Guanbin Li, Fei Wang, Yanjie Chen, Chen Qian, and Bo Li. A real-time cross-modality correlation filtering method for referring expression comprehension. In *CVPR*, pages 10880–10889, 2020. [2](#)
- [28] Haolin Liu, Anran Lin, Xiaoguang Han, Lei Yang, Yizhou Yu, and Shuguang Cui. Refer-it-in-rgbd: A bottom-up approach for 3d visual grounding in rgbd images. In *Proceedings of the IEEE/CVF Conference on Computer Vision and Pattern Recognition*, pages 6032–6041, 2021. [3](#)
- [29] Runtao Liu, Chenxi Liu, Yutong Bai, and Alan L Yuille. Clevr-ref+: Diagnosing visual reasoning with referring expressions. In *CVPR*, pages 4185–4194, 2019. [1](#)
- [30] Ilya Loshchilov and Frank Hutter. Decoupled weight decay regularization. *arXiv preprint arXiv:1711.05101*, 2017. [6](#)
- [31] Jiasen Lu, Dhruv Batra, Devi Parikh, and Stefan Lee. Vlb- bert: Pretraining task-agnostic visiolinguistic representations for vision-and-language tasks. In H. Wallach, H. Larochelle, A. Beygelzimer, F. d’Alché-Buc, E. Fox, and R. Garnett, editors, *Advances in Neural Information Processing Systems*, volume 32. Curran Associates, Inc., 2019. [1, 2](#)
- [32] Junyu Luo, Jiahui Fu, Xianghao Kong, Chen Gao, Haibing Ren, Hao Shen, Huaxia Xia, and Si Liu. 3d-sps: Single-stage 3d visual grounding via referred point progressive selection. In *CVPR*, pages 16454–16463, 2022. [1, 3, 6, 7](#)
- [33] Junhua Mao, Jonathan Huang, Alexander Toshev, Oana Camburu, Alan L Yuille, and Kevin Murphy. Generation and comprehension of unambiguous object descriptions. In *CVPR*, pages 11–20, 2016. [1, 2](#)
- [34] Varun K Nagaraja, Vlad I Morariu, and Larry S Davis. Modeling context between objects for referring expression understanding. In *ECCV*, pages 792–807. Springer, 2016. [2](#)
- [35] Myle Ott, Sergey Edunov, Alexei Baevski, Angela Fan, Sam Gross, Nathan Ng, David Grangier, and Michael Auli. fairseq: A fast, extensible toolkit for sequence modeling. In *Proceedings of NAACL-HLT 2019: Demonstrations*, 2019. [5, 6](#)
- [36] Charles R Qi, Xinlei Chen, Or Litany, and Leonidas J Guibas. Invotenet: Boosting 3d object detection in point clouds with image votes. In *CVPR*, pages 4404–4413, 2020. [3](#)
- [37] Charles R Qi, Wei Liu, Chenxia Wu, Hao Su, and Leonidas J Guibas. Frustum pointnets for 3d object detection from rgb-d data. In *CVPR*, pages 918–927, 2018. [3](#)
- [38] Charles Ruizhongtai Qi, Li Yi, Hao Su, and Leonidas J Guibas. Pointnet++: Deep hierarchical feature learning on point sets in a metric space. *Advances in neural information processing systems*, 30, 2017. [5, 6](#)
- [39] Anna Rohrbach, Marcus Rohrbach, Siyu Tang, Seong Joon Oh, and Bernt Schiele. Generating descriptions with grounded and co-referenced people. In *CVPR*, pages 4979–4989, 2017. [2](#)
- [40] Vishwanath A Sindagi, Yin Zhou, and Oncel Tuzel. Mvx-net: Multimodal voxelnet for 3d object detection. In *ICRA*, pages 7276–7282. IEEE, 2019. [3](#)
- [41] Weijie Su, Xizhou Zhu, and etc. Vi-bert: Pre-training of generic visual-linguistic representations. *arXiv preprint arXiv:1908.08530*, 2019. [2](#)
- [42] Ashish Vaswani, Noam M. Shazeer, Niki Parmar, Jakob Uszkoreit, Llion Jones, Aidan N. Gomez, Lukasz Kaiser, and Illia Polosukhin. Attention is all you need. *ArXiv*, abs/1706.03762, 2017. [2](#)
- [43] Sourabh Vora and etc. Lang. Pointpainting: Sequential fusion for 3d object detection. In *Proceedings of the IEEE/CVF conference on computer vision and pattern recognition*, pages 4604–4612, 2020. [3](#)
- [44] Peng Wang, Qi Wu, Jiewei Cao, Chunhua Shen, Lianli Gao, and Anton van den Hengel. Neighbourhood watch: Referring expression comprehension via language-guided graph attention networks. In *CVPR*, pages 1960–1968, 2019. [2](#)
- [45] Xu Yan, Jiantao Gao, Chaoda Zheng, Chaoda Zheng, Ruimao Zhang, Shenghui Cui, and Zhen Li. 2dpass: 2d priors assisted semantic segmentation on lidar point clouds. In *ECCV*, 2022. [3](#)
- [46] Sibe Yang, Guanbin Li, and Yizhou Yu. Dynamic graph attention for referring expression comprehension. In *Proceedings of the IEEE/CVF International Conference on Computer Vision*, pages 4644–4653, 2019. [1, 2](#)
- [47] Zhengyuan Yang, Tianlang Chen, Liwei Wang, and Jiebo Luo. Improving one-stage visual grounding by recursive sub-query construction. In *ECCV*, pages 387–404. Springer, 2020. [1, 2](#)
- [48] Zhengyuan Yang and etc. A fast and accurate one-stage approach to visual grounding. In *ICCV*, October 2019. [2](#)
- [49] Licheng Yu, Zhe Lin, Xiaohui Shen, Jimei Yang, Xin Lu, Mohit Bansal, and Tamara L. Berg. Mtnet: Modular attention network for referring expression comprehension. In *CVPR*, June 2018. [1, 2](#)
- [50] Licheng Yu, Patrick Poirson, Shan Yang, Alexander C Berg, and Tamara L Berg. Modeling context in referring expressions. In *ECCV*, pages 69–85. Springer, 2016. [1, 2](#)
- [51] Zhihao Yuan, Xu Yan, and etc. Instancerefer: Cooperative holistic understanding for visual grounding on point clouds through instance multi-level contextual referring. In *Proceedings of the IEEE/CVF International Conference on Computer Vision (ICCV)*, pages 1791–1800, October 2021. [1, 2](#)
- [52] Lichen Zhao, Daigang Cai, Lu Sheng, and Dong Xu. 3dvg-transformer: Relation modeling for visual grounding on point clouds. In *Proceedings of the IEEE/CVF International Conference on Computer Vision (ICCV)*, pages 2928–2937, October 2021. [1, 2, 6, 7](#)
- [53] Luowei Zhou, Yannis Kalantidis, and etc. Grounded video description. In *CVPR*, pages 6578–6587, 2019. [2](#)
- [54] Chaoyang Zhu, Yiyi Zhou, Yunhang Shen, Gen Luo, Xingjia Pan, Mingbao Lin, Chao Chen, Liujuan Cao, Xiaoshuai Sun, and Rongrong Ji. Seqtr: A simple yet universal network for visual grounding. *arXiv preprint arXiv:2203.16265*, 2022. [2](#)

- [55] Xinge Zhu, Hui Zhou, Tai Wang, Fangzhou Hong, Wei Li, Yuexin Ma, Hongsheng Li, Ruigang Yang, and Dahua Lin. Cylindrical and asymmetrical 3d convolution networks for lidar-based perception. *IEEE Transactions on Pattern Analysis and Machine Intelligence*, 44(10):6807–6822, 2021. [2](#)
- [56] Zhuangwei Zhuang, Rong Li, Kui Jia, Qicheng Wang, Yuanqing Li, and Mingkui Tan. Perception-aware multi-sensor fusion for 3d lidar semantic segmentation. In *ICCV*, pages 16280–16290, October 2021. [3](#)